NASA TECHNICAL NOTE

NASA TN D-6806

FREQUENCY RESPONSE OF A VAPORIZATION PROCESS TO DISTORTED ACOUSTIC DISTURBANCES

by Marcus F. Heidmann

Lewis Research Center
Cleveland, Ohio 44135

NATIONAL AERONAUTICS AND SPACE ADMINISTRATION • WASHINGTON, D. C. • MAY 1972

1. Report No.
NASA TN D-6806

2. Government Accession No.

3. Recipient's Catalog No.

4. Title and Subtitle
FREQUENCY RESPONSE OF A VAPORIZATION PROCESS TO DISTORTED ACOUSTIC DISTURBANCES

5. Report Date
May 1972

6. Performing Organization Code

7. Author(s)
Marcus F. Heidmann

8. Performing Organization Report No.
E-6761

9. Performing Organization Name and Address
Lewis Research Center
National Aeronautics and Space Administration
Cleveland, Ohio 44135

10. Work Unit No.
113-31

11. Contract or Grant No.

12. Sponsoring Agency Name and Address
National Aeronautics and Space Administration
Washington, D.C. 20546

13. Type of Report and Period Covered
Technical Note

14. Sponsoring Agency Code

15. Supplementary Notes

16. Abstract

The open-loop response properties expressed as the mass vaporized in phase and out of phase with the pressure oscillations were numerically evaluated for a vaporizing n-heptane droplet. The evaluation includes the frequency dependence introduced by periodic oscillation in droplet mass and temperature. A given response was achieved over a much broader range of frequency with harmonically distorted disturbances than with sinusoidal disturbances. The results infer that distortion increases the probability of incurring spontaneous and triggered instability in any rocket engine combustor by broadening the frequency range over which the vaporization process can support an instability.

17. Key Words (Suggested by Author(s))
Rocket combustion; Combustion instability; Drop vaporization; Combustion response; Combustion dynamics; Nonlinear instability; Vaporization response

18. Distribution Statement
Unclassified - unlimited

19. Security Classif. (of this report)	20. Security Classif. (of this page)	21. No. of Pages	22. Price*
Unclassified	Unclassified	33	$3.00

* For sale by the National Technical Information Service, Springfield, Virginia 22151

FREQUENCY RESPONSE OF A VAPORIZATION PROCESS TO DISTORTED ACOUSTIC DISTURBANCES

by Marcus F. Heidmann

Lewis Research Center

SUMMARY

The open-loop frequency response properties of a drop vaporization process were numerically evaluated for acoustic disturbances with harmonically distorted wave shapes (wave shapes which deviated from pure sinusoidal forms). A single-drop model was used which allows for oscillations in drop mass and temperature. Calculations were made for n-heptane droplets vaporizing in oxygen under simulated unstable rocket combustor conditions. Response factors expressing the mass vaporized in phase and out of phase with the pressure oscillations were evaluated over a broad range of frequencies for a variety of harmonically distorted disturbances.

For sinusoidal oscillations, typical response properties of the vaporization process were obtained with the single-drop model. The in-phase response factor increased from zero at low frequencies to a peak value at some intermediate frequency and then decreased to a large negative value at high frequencies. Harmonic distortion was found to substantially affect these in-phase response properties. In some instances the peak response was increased by an order of magnitude above that for sinusoidal disturbances. In general, the response factor increased by a constant increment for all frequencies at and above that for peak response. At low frequencies the response always decreased to zero. Effects of comparable magnitude were found for the out-of-phase response factor, but they occurred at different frequency conditions.

The effect of harmonic distortion on the peak in-phase response factor was equivalent to that reported for a vaporization model which neglected the frequency-dependent behavior associated with drop mass and temperature oscillations. That study concluded that harmonic distortion can cause or contribute to the instability in rocket combustors. The present study for the frequency-dependent process gives the same conclusions. The present analysis also shows that harmonic distortion can substantially broaden the frequency range over which the vaporization process can support unstable combustion.

INTRODUCTION

A previous study (ref. 1) showed that the manner in which a vaporizing drop responds to an acoustic disturbance is highly dependent on the wave shape of the disturbance. Harmonic distortion (deviations from sinusoidal wave shapes) was found to substantially affect those response properties which control the stability of combustion systems. The study qualitatively showed that the harmonic distortion in a disturbance can cause or contribute to combustion instability problems in liquid-propellant rocket engines and provided some insight into the design of stable combustors. These results were obtained by neglecting the frequency-dependent behavior of the vaporization process. The present study extends the analysis into the frequency domain. The purpose of the study is (1) to verify the deductions of the previous study with a frequency-sensitive vaporization model and (2) to relate to combustor stability problems any changes in frequency-dependent behavior caused by wave distortions.

The vaporization model used in the previous study of response properties (ref. 1) considered vaporization rate to be simply proportional to the drop Reynolds number to an exponential power. Such a quasi-steady model will provide no frequency-dependent behavior, whereas the response of the vaporization process has been shown to be highly frequency dependent (refs. 2 and 3). The sensitivity to frequency is caused by mass and thermal time lags; that is, a change in the vaporizing environment does not cause an instantaneous change in the drop mass and temperature. A model which includes a heat and mass balance for the vaporizing liquid drop is needed to give these time-lag properties. The present study uses such a model.

The dynamic behavior of this vaporization process (model) is numerically analyzed in this study. The specific process examined is n-heptane droplets vaporizing in gaseous oxygen under simulated rocket combustion conditions. Calculations are made of the instantaneous vaporization rates caused by assumed acoustic disturbances (open-loop analysis). Evaluations are made over a broad range of frequencies for a variety of harmonically distorted disturbances. The calculated oscillations in vaporization rate are expressed in terms of response properties which describe the relation between the vaporization rate and acoustic oscillations. The results are discussed within the content of the previous studies and with regard to their application to rocket combustors.

The response properties used in this study to relate vaporization rate oscillations to harmonically distorted acoustic oscillations require some clarification. These response properties are expressed as two quantities: the in-phase and out-of-phase response factors. These response factors are the in-phase and out-of-phase components of the vaporization rate oscillations relative to the acoustic pressure oscillations, where both oscillations are given as fractional perturbations about the mean value of the variable. The components are extracted directly from the distorted oscillations by a corre-

lation procedure which accounts for any contribution caused by harmonic content in the oscillations. Justification for such nonlinear evaluations of the response factors is given in reference 1. The basic significance of the response factors to combustion instability problems has evolved and been adopted from linear stability analyses.

In linear (small sinusoidal) analyses the relation between two periodic variables is readily expressed either in terms of a phase angle and amplitude ratio or in terms of in-phase (real) and out-of-phase (imaginary) components. Both notations are interrelated, but the in-phase and out-of-phase components have received most attention in combustor stability analyses. In stability analyses of combustor systems the boundary conditions characterizing the combustion process are specified by the in-phase and out-of-phase components of the burning rate oscillations relative to the pressure oscillations. Both components (response factors) are needed to determine the stability characteristics of any specific combustion system.

Systems analyses such as reference 4 show that the periodic behavior of any system is, in general, related to the properties of the response factors. The amplitude of sustained oscillations will increase with an increase in the in-phase response factor, and sustained oscillations will usually occur when the in-phase response factor exceeds a threshold value of about unity. The in-phase response factor, therefore, can be used as a qualitative index of the stability of a rocket combustor system. The out-of-phase response factor mainly controls the frequency of sustained oscillations. The frequency increases with an increase in the out-of-phase response factor.

SYMBOLS

c	speed of sound, m/sec; ft/sec
H^*	drop enthalpy, $H/\overline{H}$
$\mathcal{I}$	out-of-phase response factor, eq. (10)
m^*	drop mass, $m/\overline{w}$
n	harmonic order
P^*	environmental pressure, $P/\overline{P}$
P_v^*	drop vapor pressure, $P_v/\overline{P}$
p_1, p_2	harmonic coefficients for pressure disturbance ($p_1 < 1.0$), dimensionless
q^*	heat transfer rate, $q/\overline{wH}$
$\mathcal{R}$	in-phase response factor, eq. (9)
r	drop radius, μm

r_o initial drop radius, μm

t time, sec

u transverse gas velocity, m/sec; ft/sec

$\Delta\overline{v}$ steady relative axial drop velocity, m/sec; ft/sec

w* drop vaporization rate, $w/\overline{w}$

γ ratio of specific heats

θ phase relation between velocity and pressure disturbance

λ* heat of vaporization, $\lambda/\overline{H}$

τ characteristic drop lifetime, $m/\overline{w}$, sec

φ phase relation between harmonic components of disturbance

ω frequency, rad/sec

Superscripts:

( )' primed quantities denote dimensionless perturbations, $X' = \frac{x - \overline{x}}{\overline{x}}$

($\overline{\ }$) barred quantities denote mean values

OPEN-LOOP MODEL

The response properties of the vaporization process are obtained by an open-loop analysis by which the perturbations in vaporization rate caused by assumed acoustic oscillations are evaluated and correlated.

Vaporization Process

The vaporization model used in this study closely follows that developed in reference 5 for vaporization-limited combustion in liquid-propellant rocket combustors. The model is applied in a manner similar to that used in reference 3 for a linear analysis of the frequency response properties of the vaporization process. The linear analysis showed that a single-drop model can adequately characterize the entire vaporization process with its multiplicity of drops. The single-drop model must, however, account for the continuous injection of propellant which occurs in combustors and which is an important source of frequency-dependent behavior. A steady liquid flow into a single drop simulates the dynamic effect of continuous propellant injection into a combustor. The single-drop model used previously and in this study is comparable to experimental

models where a single drop is suspended and continuously supplied by a hypodermic needle.

The following sketch depicts the analytical model:

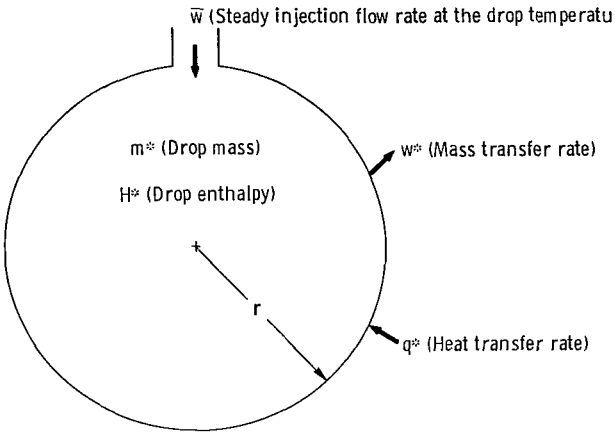

A vaporizing drop of radius r is continuously supplied by a steady flow rate $\overline{w}$. The heat transfer rate q* to the drop causes a vaporization rate w*. The total heat and mass transferred establishes the instantaneous drop mass m* and the drop enthalpy H*.

The analysis of response properties is restricted to equilibrium conditions of vaporization. For vaporization in a steady environment, an equilibrium condition of heat and mass transfer exists, where none of the vaporization variables change with time. At equilibrium there is a specific drop radius for each steady injected flow rate which satisfies a given heat and mass balance. A comparable condition exists for vaporization in a perturbed environment where the flow field varies periodically at a constant frequency and amplitude. In this case the drop radius and the heat and mass transfer vary periodically about some mean value. At equilibrium the oscillations about the mean do not vary from one period to the next. This condition of periodic equilibrium is specifically analyzed in this study.

An analysis is made of n-heptane vaporizing in gaseous oxygen at simulated rocket combustor conditions. The vaporization equations and physical properties given in reference 5 are used. The specific equations used in this study (expressed in normalized parameters and including physical properties) are developed in appendix A and given by the following relations:

(1) Vaporization rate

$$w^* = c_1 \frac{(\Delta\bar{v}/100)^{1/2}}{(r_o/100)^{3/4}} (P^*)^{1/2}(m^*)^{1/2}\left[1 + \left(\frac{u}{\Delta\bar{v}}\right)^2\right]^{1/4} \ln\left(\frac{P^*}{P^* - P_v^*}\right) \tag{1}$$

where c_1 equals 60 and 33, respectively, for $\Delta\bar{v}$ given in meters per second and feet per second

(2) Heat transfer rate

$$q^* = c_2 \frac{(\Delta\bar{v}/100)^{1/2}}{(r_o/100)^{3/4}} (P^*)^{1/2}(m^*)^{1/2}\left[1 + \left(\frac{u}{\Delta\bar{v}}\right)^2\right]^{1/4} \frac{\ln\left(\frac{P^*}{P^* - P_v^*}\right)}{\left(\frac{P^*}{P^* - P_v^*}\right)^{6.15} - 1} \tag{2}$$

where c_2 equals 363 and 200, respectively, for $\Delta\bar{v}$ given in meters per second and feet per second

(3) Enthalpy balance

$$\frac{dH^*}{dt} = \frac{1}{m^*}(q^* - w^* \lambda^*) \tag{3}$$

(4) Mass balance

$$\frac{dm^*}{dt} = 1 - w^* \tag{4}$$

The vapor pressure and heat of vaporization properties of n-heptane were curve fitted to give

$$P_v^* = e^{7-(7.8/H^*)} \tag{5}$$

$$\lambda^* = 0.65 - \frac{H^*}{2} \tag{6}$$

The coefficients for the vaporization-rate and heat-transfer-rate expressions are given for a condition of equilibrium vaporization in a steady environment. The condition used is a drop radius r_o of 100 micrometers, a steady relative axial velocity between the

drop and gas Δv of 30.5 meters per second (100 ft/sec), and a combustor pressure of 2068 kN/m^2 (300 psia). At these conditions w^*, q^*, and H^* are equal to unity. The variable m^* is actually the characteristic drop lifetime ($m^* = m/\overline{w} = \tau$) and is not equal to unity.

Acoustic Oscillations

The acoustic oscillations used to perturb the vaporization process are identical to those assumed for some specific evaluations of reference 1 with which the results of this study will be compared. The oscillations in pressure and acoustic particle velocity which describe the acoustic disturbances are assumed to be similarly distorted. The distortion consists of harmonic components which are added to a fundamental oscillation. Distortion is varied by changes in the magnitude and phase of the harmonic components relative to the fundamental. Two types of distorted oscillations are examined.

(1) Second harmonic distortion

$$\left.\begin{aligned} P^{*\prime} &= p_1\left[\cos\ \omega t + \frac{p_2}{p_1}\cos(2\omega t - \varphi)\right] \\ u &= \frac{cp_1}{\gamma}\left[(\cos\ \omega t - \theta) + \frac{p_2}{p_1}\cos(2\omega t - \varphi - \theta)\right] \end{aligned}\right\} \tag{7}$$

(2) Multiharmonic distortion

$$\left.\begin{aligned} P^{*\prime} &= \sum_{n=1}^{\infty} p_1^n \cos(n\omega t - \varphi) \\ u &= \frac{c}{\gamma}\sum_{n=1}^{\infty} p_1^n \cos(n\omega t - \varphi - \theta) \end{aligned}\right\} \tag{8}$$

The phase angles φ and θ express, respectively, the phase relation between the harmonic components and the phase relation between velocity and pressure. Equation (8) characterizes high-amplitude oscillations observed in unstable rocket combustors, where the amplitude of the harmonic component usually decreases exponentially with harmonic order, that is, $p_n = p_1^n$.

Response Factors

Two response factors (more fully discussed in the INTRODUCTION and in ref. 1) are evaluated to express the mass vaporized in-phase and out-of-phase with the pressure oscillation. The correlation procedure used to evaluate the response factors is given by the following expressions:

(1) In-phase response factor $\mathcal{R}$

$$\mathcal{R} = \frac{\int_0^{2\pi} P^{*\prime} w^{*\prime} \, d\omega t}{\int_0^{2\pi} (P^{*\prime})^2 \, d\omega t} \tag{9}$$

(2) Out-of-phase response factor $\mathcal{I}$

$$\mathcal{I} = \frac{\int_0^{2\pi} w^{*\prime} P^{*\prime}_{(\omega t + \pi/2)} \, d\omega t}{\int_0^{2\pi} (P^{*\prime})^2 \, d\omega t} \tag{10}$$

METHOD OF ANALYSIS

Numerical Solutions

The response factors were evaluated by numerical procedures for the finite amplitude disturbances. A desk-top calculator (Hewlett-Packard 9100A) with a capacity equivalent to 140 program steps and six storage registers was used. Solutions for the response factors were obtained by a convergence procedure involving cyclic repetition. The flow diagram shown in figure 1 describes the procedure.

The calculation procedure is such that an initial drop radius r_o and initial enthalpy H_o for a steady environment are known, but the mean drop radius $\bar{r}$ and mean enthalpy $\bar{H}$ for a periodic environment are not known until valid solutions for $\mathcal{R}$ and $\mathcal{I}$ are obtained. The enthalpy differs negligibly for steady and unsteady conditions, but $\bar{r}$ can be considerably smaller than r_o. The initial drop radius r_o is comparable to the drop size delivered by the propellant injector during combustion instability. Some of the results are presented as a function of this pseudo-injected drop size.

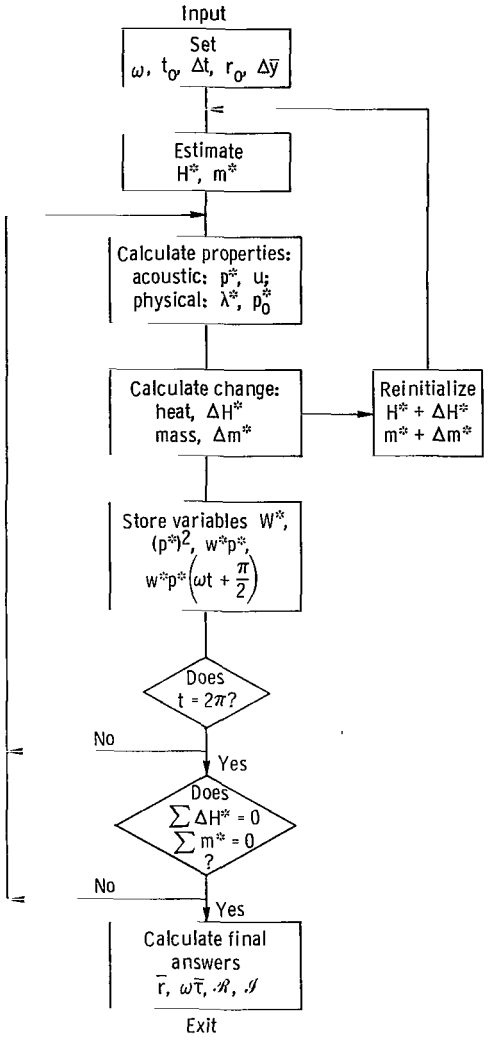

Figure 1. - Flow diagram showing convergence procedure.

Linear Analytical Solutions

Linear analytical solutions for the response factors were evaluated for comparison with the computer-generated numerical solutions at small pressure amplitudes. Linear analytical solutions for the frequency response properties of n-heptane have previously been reported in reference 3. In that study correction terms for simultaneous heat and mass transfer of the drop surface and the variation of λ (heat of vaporization) were neglected. Appendix B of this report presents a linear analysis which follows the method of reference 2 but includes these additional variables.

The transfer function which applies specifically to this study as derived in appendix B is given by

$$\frac{w^{*\prime}}{p^{*\prime}} = 0.622 \frac{2\bar{m}^* S}{1 + 2\bar{m}^* S} \left(\frac{1 - 0.249\ \bar{m}^* S}{1 + 0.178\ \bar{m}^* S} \right)$$

The response factors $\Re$ and $\mathcal{I}$ are the real and imaginary parts of $w^{*\prime}/P^{*\prime}$, where $S = i\omega$.

RESULTS AND DISCUSSION

Harmonic distortion in the acoustic oscillations affected the frequency response properties of the vaporization process in a similar manner for both types of distortion. This general effect of distortion on the frequency response is described first. Some results follow for specific variations in second harmonic and multiharmonic distortion similar to those used in the quasi-steady analysis of reference 1.

General Effect of Distortion

A general effect of harmonic distortion on the frequency response observed for all types of distortion is illustrated in figure 2. The in-phase response factor $\Re$ is shown as a function of frequency for both sinusoidal oscillations ($p_2/p_1 = 0$) and for oscillations distorted by second harmonic content ($p_2/p_1 = 0.2$) under otherwise identical conditions. The sinusoidal oscillations give the typical frequency response properties reported previously (refs. 2 and 3). The response increases from zero at low frequencies to a peak value at intermediate frequencies and then decreases to a constant negative value at high frequencies. Although the response always decreases to zero at low frequencies, figure 2 shows that harmonic distortion generally elevates the response curve above that for sinusoidal disturbances. Distortion increases the response factor by a relatively constant increment for frequencies at and above that for the peak value of the response factor, implying an additive rather than amplifying effect of distortion on response. The amount of the incremental increase is nearly identical to that obtained for comparable conditions of distortion in the quasi-steady analysis of reference 1.

General agreement is exhibited between the results of this study and that of reference 1 concerning the increase in the in-phase response factor caused by harmonic distortion. The conclusions stated in reference 1 regarding the effect of distortion on the peak response appear valid and the consequences of changes in the in-phase response factor on combustor stability extensively discussed in reference 1 will not be reiterated in this report. Some additional conclusions regarding frequency-dependent behavior, however, can be drawn from the present study. In particular, figure 2 shows that har-

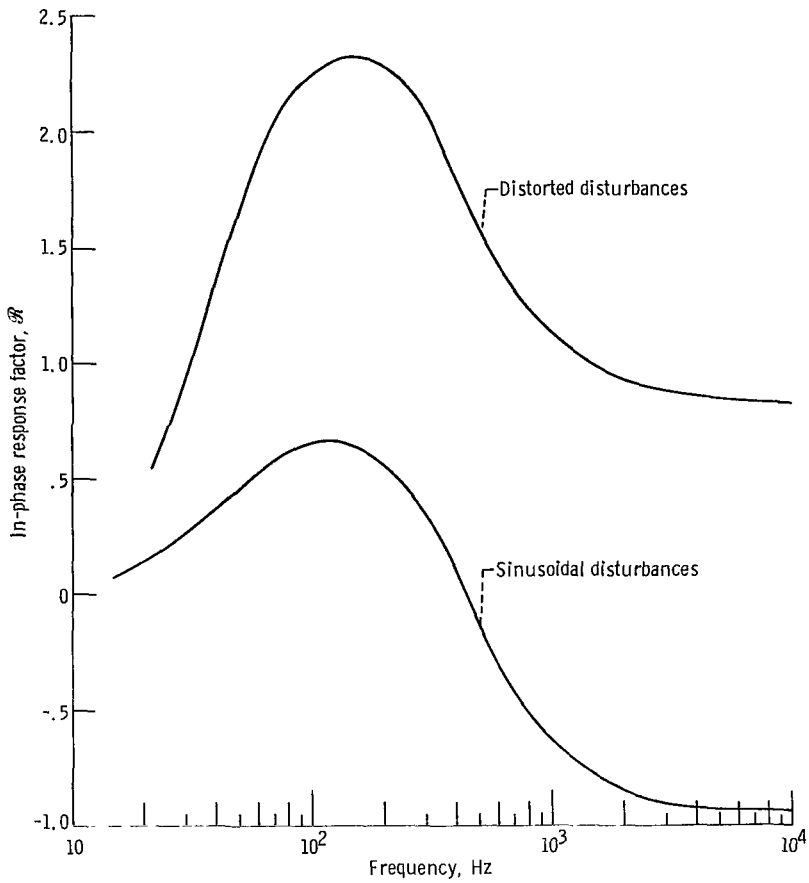

Figure 2. - Characteristic effect of wave distortion on in-phase response factor. Conditions: initial drop radius r_0, 100 μm; relative axial Mach number $\Delta\overline{v}/c$, 0.02; pressure amplitude P'_{rms}, 0.02; ratio of harmonic coefficients p_2/p_1, 0.2 for distorted disturbances and 0 for sinusoidal disturbances.

monic distortion can broaden the frequency range over which any vaporization process can cause instability. For example, if a value of $\Re$ greater than 0.6 will cause instability in a particular combustor, figure 2 shows that the instability can only occur at a frequency of 100 hertz with sinusoidal oscillations, whereas it can occur at any frequency larger than 20 hertz with the distorted oscillations.

Harmonic distortion also affects the out-of-phase response factor $\mathcal{I}$, but the effect is less readily generalized than that for the in-phase response factor $\Re$. The effect of distortion in $\mathcal{I}$ is best described by examining the response properties in the complex plane of $\Re$ and $\mathcal{I}$ shown in figure 3. The response curve for sinusoidal oscillations ($p_2/p_1 = 0$) is typical of that used as the boundary condition for vaporization-limited combustion to obtain stability solutions for rocket combustor systems (ref. 4). The value of $\mathcal{I}$ is shown to vary between 0.2 and -0.85. The value of $\mathcal{I}$ is zero when $\Re$ is a maximum. For the condition of $p_2/p_1 = 0.2$ (identical condition for that of fig. 2)

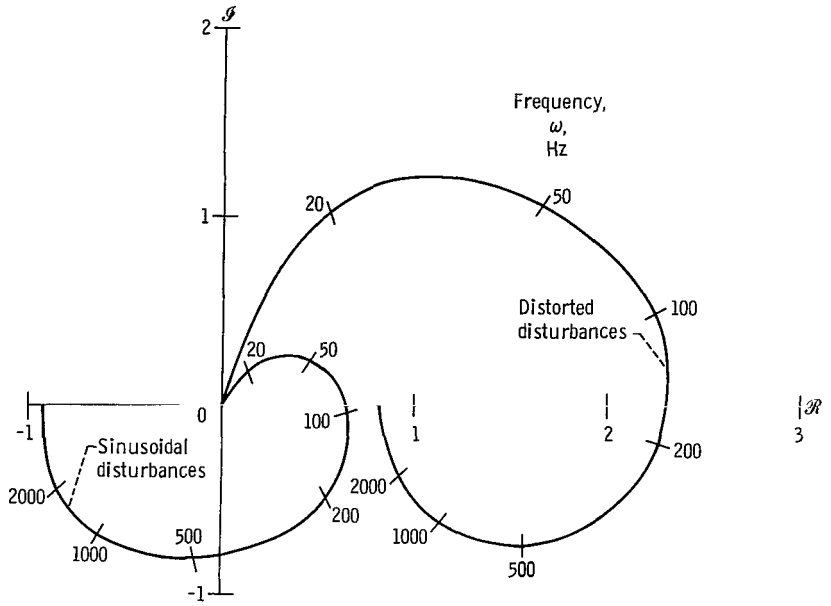

Figure 3. - Characteristic effect of wave distortion on frequency response properties in complex plane. Conditions: initial drop radius r_0, 100 μm; relative axial Mach number $\Delta\bar{v}/c$, 0.02; pressure amplitude P'_{rms}, 0.02; ratio of harmonic coefficients p_2/p_1, 0.2 for distorted disturbances and 0 for sinusoidal disturbances.

the distortion mostly affects $\mathcal{I}$ at frequencies less than that for the peak value of $\mathcal{R}$, and the effect is substantial. The most important effect of distortion on the response curve in the $\mathcal{R}$, $\mathcal{I}$ plane is the translation in the $\mathcal{R}$-coordinate caused by the additive effect of distortion on $\mathcal{R}$ noted in figure 2. The change in $\mathcal{I}$, however, is not insignificant with regard to instability in rocket combustors. Any increase in the area encompassed by the response curve in the $\mathcal{R}$, $\mathcal{I}$ plane increases the number of combustion chamber configurations which will give periodic solutions (instability) with a particular vaporization process.

The specific effect of distortion on the response curve in the $\mathcal{R}$, $\mathcal{I}$ plane may differ from that shown in figure 3 for other conditions. Generally, distortion increases the area encompassed by the response curve and increases the prospect for unstable combustion.

Another generalization can be drawn from the results of the analysis which is not specifically related to harmonic distortion in the acoustic disturbances. Rather, it is a general behavior related to the amplitude of the disturbance. Figure 4 shows the general effect of pressure amplitude on the in-phase response curve for both distorted and sinusoidal disturbances. In addition to the change in the magnitude of the response factor, figure 4(a) shows that the frequency at which the response attains a peak value increases with an increase in pressure amplitudes. This effect was also noted in reference 2. The peak response frequency increases because the mean drop size, which

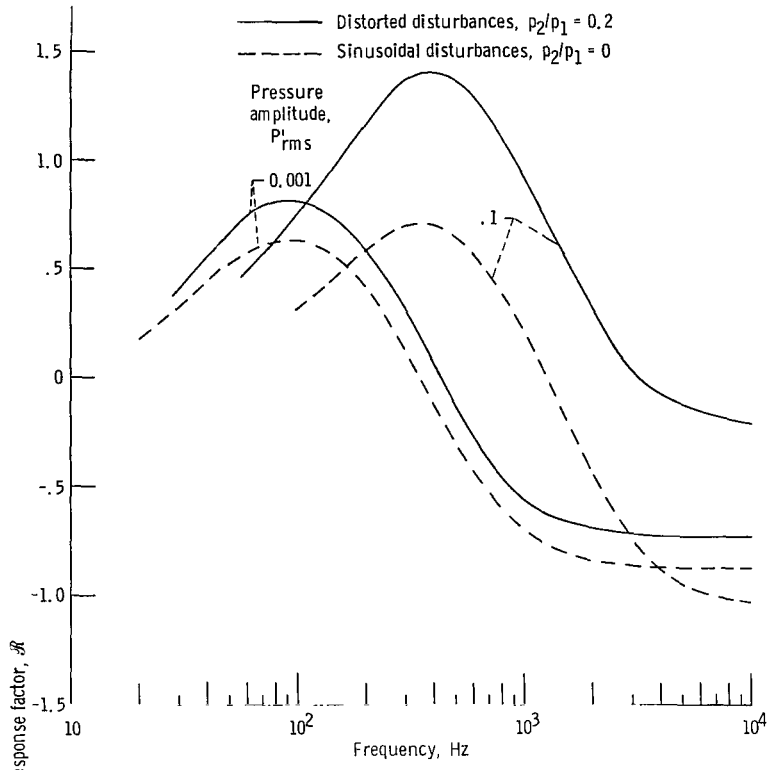

(a) Variation with frequency.

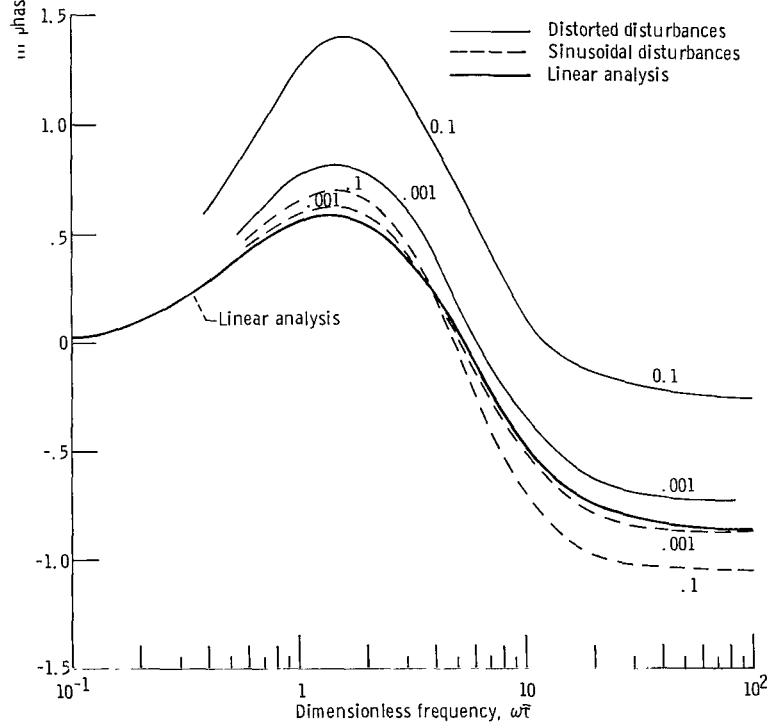

(b) Correlation with dimensionless frequency.

Figure 4. - Effect of pressure amplitude on response properties. Conditions: initial drop radius r_0, 100 μm; relative axial Mach number $\Delta\bar{v}/c$, 0.02.

characterizes that of an entire spray, decreases with an increase in the amplitude of the acoustic oscillations. The smaller drop size can respond more quickly to a change in the environment and thus shifts the peak response to a higher frequency region.

The average change in drop size with pressure amplitude is shown in figure 5. This change in drop size with pressure amplitude is relatively independent of the amount of harmonic distortion when the amplitude is expressed (as in fig. 5) as a root-mean-square value. Also shown in figure 5 is the characteristic drop lifetime $\overline{\tau}$, or its equivalent $\overline{m}^*$, which is proportional to the cube of the drop radius. The characteristic drop lifetime is used in the dimensionless frequency $\omega\overline{\tau}$, which is provided by linear

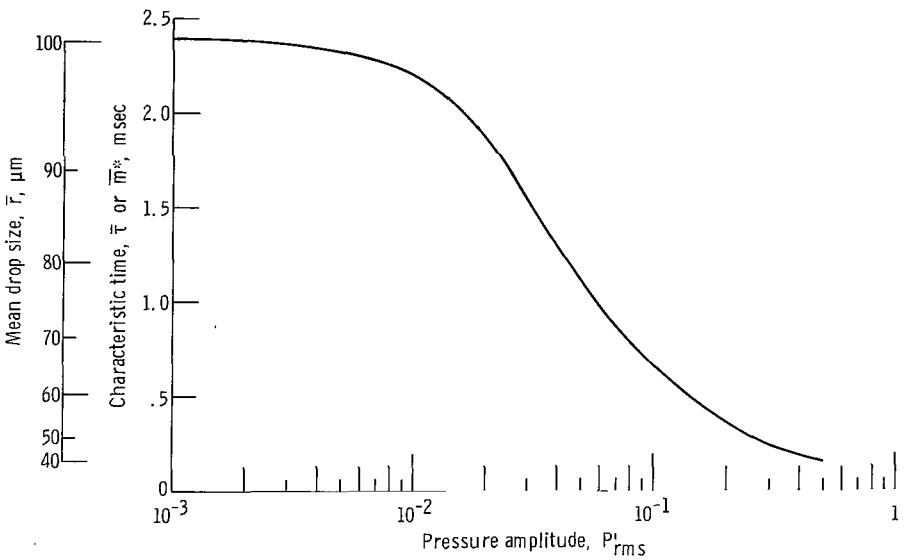

Figure 5. - Effect of pressure amplitude on mean drop size and characteristic time. Conditions: initial drop size r_0, 100 μm; relative axial Mach number $\Delta\overline{w}/c$, 0.02.

analyses (appendix B and ref. 3) as a correlation parameter for frequency response properties. The response properties of figure 4(a) are shown as a function of this dimensionless frequency in figure 4(b). The parameter correlates the results such that peak response for all conditions occurs at an $\omega\overline{\tau}$ of about 1.5.

Figure 3(b) also shows the linear solution for the in-phase response factor, which can be compared with the numerical solution for low-amplitude sinusoidal disturbances. Appendix C shows that the numerical solutions converge on the analytical solutions at extremely low amplitude and provide a degree of confidence in the numerical solution techniques. This is examined more thoroughly in appendix C.

The shift in the frequency for peak response with pressure amplitude noted in figure 3 implies that disturbances of a certain amplitude may trigger instability in a combustor by virtue of the frequency shift rather than by a change in the magnitude of the

peak response. For example, the natural resonant frequency of a combustor may be much larger than the frequency for peak response at small pressure amplitudes. An increase in pressure amplitude, however, could increase the peak response frequency until it matches the resonant frequency and thereby cause instability. Rocket combustors are often subjected to dynamic stability tests by introducing disturbances of increasing amplitude and harmonic distortion in the combustion chamber. A certain disturbance may cause instability not only because the distortion increased the in-phase response factor, but also because the amplitude of the disturbance shifted the peak response frequency. Figure 4 shows that a pressure amplitude of 0.1 will increase the frequency for peak response by a factor of 6 above that for infinitesimal disturbances.

Additional Effects of Harmonic Distortion

In reference 1, second harmonic distortion produced a maximum in-phase response factor for particular values of second harmonic content and pressure amplitude. The frequency response properties exhibit a similar behavior. Figures 6(a) and (b) show the effect of pressure amplitude on the in-phase response factor $\mathcal{R}$ for disturbances distorted by a constant amount of second harmonic content (p_2/p_1 = constant). Figure 7 shows the effect of the amount of second harmonic content at a constant pressure amplitude. Maximum response is shown to occur at a pressure amplitude of about 0.02 with a second harmonic content p_2/p_1 of 0.8. This maximum response is about an order of magnitude larger than that for sinusoidal disturbances ($p_2/p_1 = 0$).

The effect of a change in the harmonic phase angle φ and the velocity-pressure phase angle θ is shown in the $\mathcal{R}$, $\mathcal{I}$ plane in figure 8. An increase in these phase angles usually decreases both $\mathcal{R}$ and $\mathcal{I}$ and thus decreases the probability of incurring instability.

Multiharmonic distortion (eq. (8)) affects the frequency response properties, as shown in figure 9 and 10. Harmonic distortion increases with pressure amplitude and affects the pressure wave shape, as shown by the insert in figure 9. As inferred in reference 1, the peak in-phase response factor is shown to increase with an increase in pressure amplitude and to approach asymptotically a maximum value of about 1.4. The peak response frequency also increases with pressure amplitude. The effect of pressure amplitude on the response properties in the $\mathcal{R}$, $\mathcal{I}$ plane is shown in figure 10. The general effect of multiharmonic distortion on these response properties is similar to that caused by second harmonic distortion.

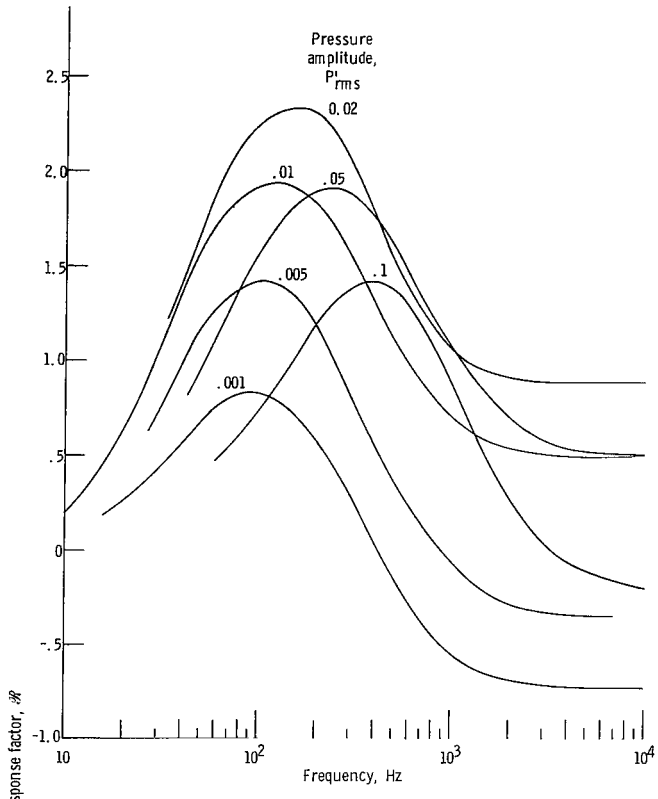

(a) Variation with frequency.

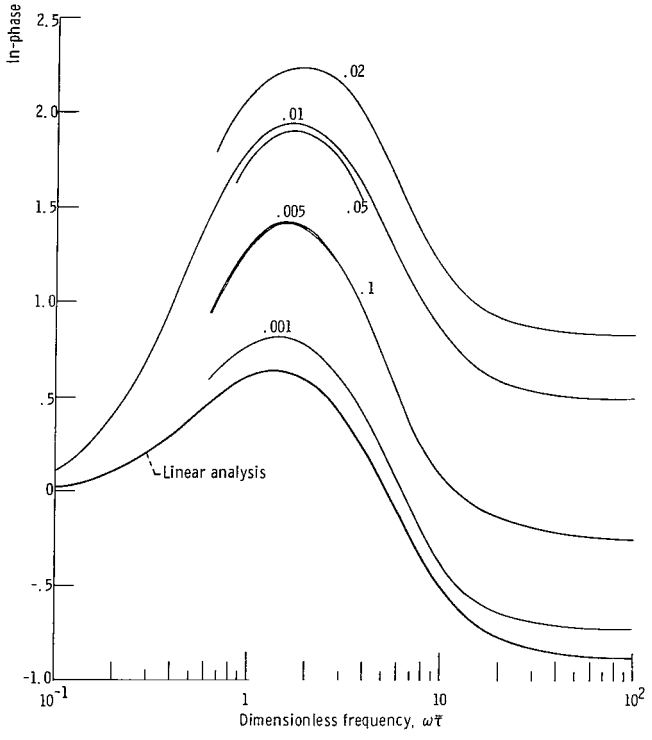

(b) Correlation with dimensionless frequency.

Figure 6. - Effect of pressure amplitude on in-phase response factor for disturbances with constant distortion. Conditions: initial drop radius r_0, 100 μm; relative axial Mach number $\Delta\bar{w}/c$, 0.02; ratio of harmonic coefficients p_2/p_1, 0.2.

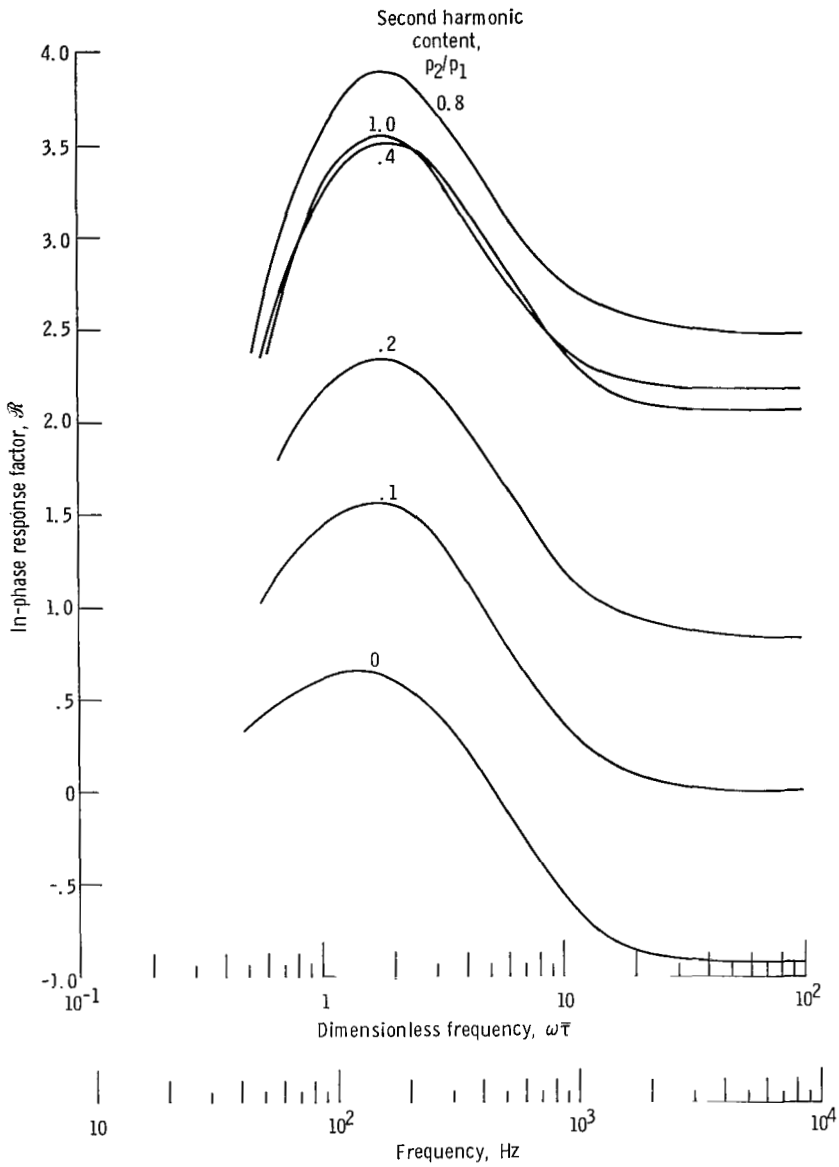

Figure 7. - Effect of second harmonic content on in-phase response factor. Conditions: initial drop radius r_0, 100 μm; relative axial Mach number $\Delta\bar{v}/c$, 0.02; pressure amplitude P'_{rms}, 0.02.

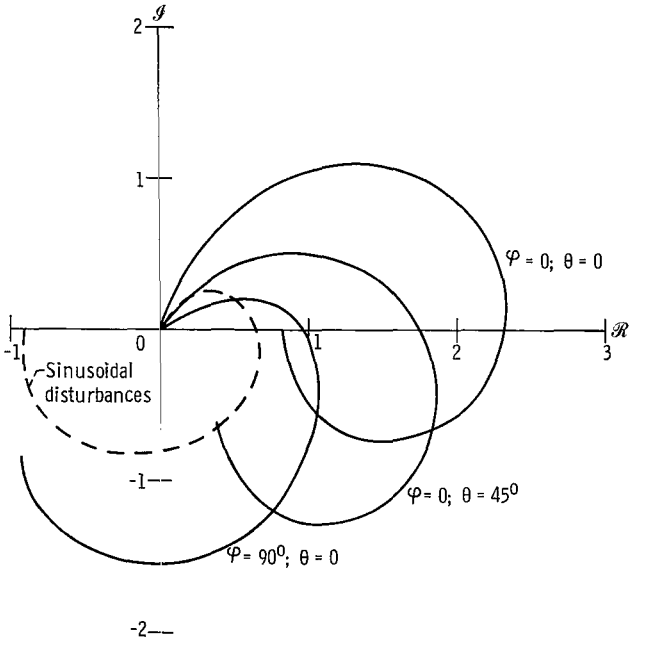

Figure 8. - Effect of harmonic phase angle and velocity-pressure phase angle on response properties. Conditions: initial drop radius r_0, 100 μm; relative axial Mach number $\Delta\bar{v}/c$, 0.02; ratio of harmonic coefficients p_2/p_1, 0.2; pressure amplitude P'_{rms}, 0.02.

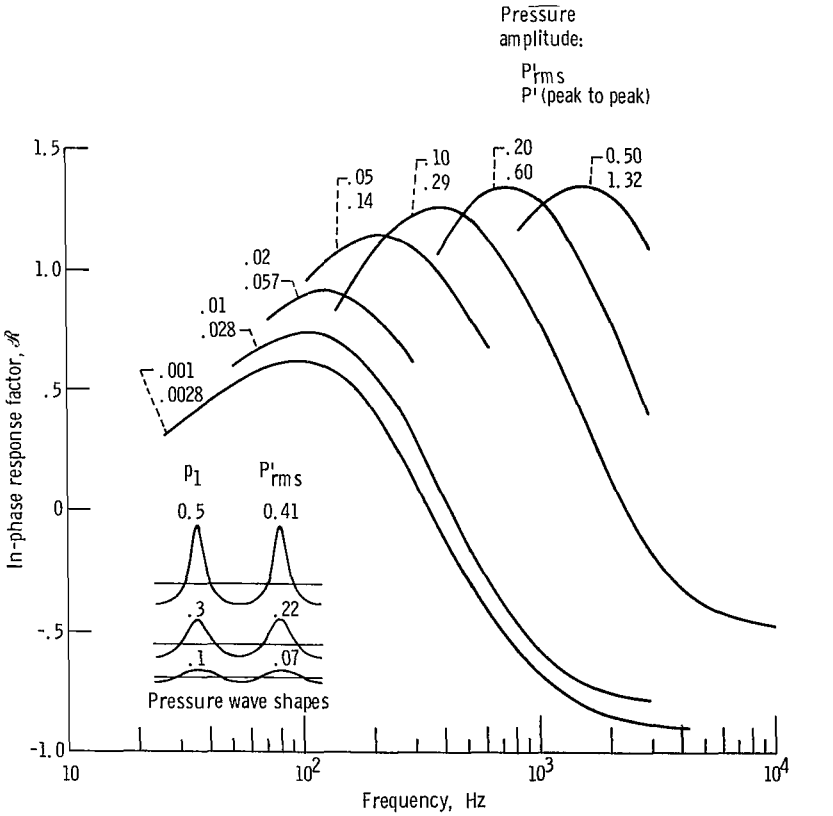

Figure 9. - Effect of pressure amplitude on in-phase response factor for multiharmonic disturbances. Conditions: relative axial Mach number $\Delta\bar{v}/c$, 0.02; $P' = \sum_{n=1}^{\infty} p_1^n \cos n\omega t$.

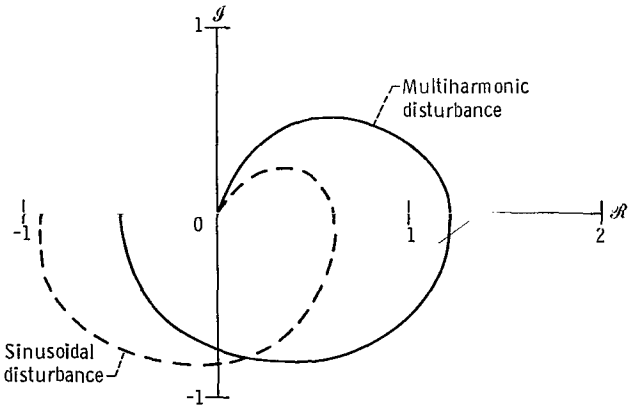

Figure 10. - Comparison of response properties for multiharmonic and sinusoidal disturbances. Conditions: initial drop radius r_0, 100 μm; relative axial Mach number $\Delta\bar{w}/c$, 0.02; pressure amplitude P'_{rms}, 0.1.

SUMMARY OF RESULTS

The results of this numerical analysis of the effect of wave distortion on the response properties of a frequency-dependent n-heptane vaporization process are summarized as follows:

1. The amplifying effect of wave distortion on the response properties obtained by a previous analysis using a quasi-steady vaporization model were confirmed by the frequency-dependent model. The in-phase response factor exhibited substantial increases in peak response as predicted by the quasi-steady analysis. At frequencies higher than that for peak response, harmonic distortion increased the in-phase response factor by an increment equal to that for the peak response. At low frequencies the response always approached a value of zero. The frequency for peak response increased with the root-mean-square amplitude of the pressure oscillation. The increase was relatively independent of the type of harmonic distortion. The out-of-phase response factor was mostly affected at a frequency less than that for peak in-phase response.

2. The results imply that the effects of harmonic distortion deduced from the quasi-steady analysis with regard to increasing the probability of spontaneous and triggered instability in rocket combustors are equally applicable for the frequency-dependent process. In addition to these previous effects concerned with the magnitude of the response factors, this study shows important changes in frequency characteristics. Distortion can substantially increase the range of frequencies in which the vaporization process can support combustion instability and can shift the frequency for peak response to match

the resonant frequency of a combustion chamber. In general, distortion increases the number of combustor configurations which can be unstable for a particular combustion process.

Lewis Research Center,
National Aeronautics and Space Administration,
Cleveland, Ohio, March 13, 1972,
113-31.

APPENDIX A

VAPORIZATION EQUATIONS

In this appendix equations for the vaporization process are developed for drops which are at or near their equilibrium temperature. The vaporization model and physical properties given in reference 5 are used for this purpose. The propellant combination is n-heptane and gaseous oxygen. For convenience, an English system of units generally following that of reference 5 is used in developing the normalized equations.

Physical Properties and Special Symbols

The physical properties of the n-heptane - oxygen mixture surrounding the drop are assumed to be unaffected by changes in the drop temperature. Specifically, they are evaluated for a drop temperature of 845° R (equilibrium temperature for a chamber pressure of 300 psi) and a mean gas temperature in the drop boundary of 2000° R. The physical properties evaluated at these conditions and the dimensional symbols used in this appendix are given by the following notations:

$(C_p)_v$ specific heat of heptane vapor, 0.9365 Btu/(lb)($^{\circ}$R)

$(C_p)_l$ specific heat of heptane liquid, 0.70589 Btu/(lb)($^{\circ}$R)

$(C_p)_m$ specific heat of gas mixture, 0.641 Btu/(lb)($^{\circ}$R)

D molecular diffusion coefficient of gas mixture, 7.492×10^{-3} (300/P) in.^{2}/sec

H drop enthalpy, Btu/lb

k thermal conductivity of gas mixture, 6.673×10^{-7} Btu/(in.)(sec)($^{\circ}$R)

M_m molecular weight of gas mixture, 46.3 lb/mole

M_v molecular weight of heptane, 100 lb/mole

$P, \bar{P}$ total pressure, lb/in.^{2}; $\bar{P}$ = 300 psi

P_v vapor pressure of heptane, $300\, e^{7-\left[4670/(C_p)_l T_l\right]}$ psi

Pr Prandtl number, $(C_p)_m \mu/k$ = 2.912, dimensionless

q heat transfer rate, Btu/sec

R universal gas constant, 1545 (ft)(lbf)/($^{\circ}$R)(lb)(mole)

Re	Reynolds number, $2rU\rho_m/\mu = 3.94\times10^{-4}\,rPU$, dimensionless
r	drop radius, μm
Sc	Schmidt number, $\mu/D\rho_m = 1.0788$, dimensionless
$\overline{T}$	gas mixture temperature, 2000° R
T_g	combustion gas temperature, $^{\circ}$R
T_l	drop temperature, $^{\circ}$R
t	time, sec
U	magnitude of relative drop velocity, ft/sec
u	transverse gas velocity, ft/sec
$\Delta\overline{v}$	steady relative axial drop velocity, ft/sec
w	vaporization rate, lb/sec
Z, z	correction terms for heat transfer, eq. (A6)
λ	heat of vaporization of heptane, $392 - \left(C_p\right)_l T_l/2$ Btu/lb
μ	viscosity of gas mixture, 3.033×10^{-6} lb/(in.)(sec)($^{\circ}$R)
ρ_l	density of heptane liquid, 1.8646×10^{-2} lb/in.^{3}
ρ_m	density of gas mixture, $3.76\times10^{-4}(P/300)$ lb/in.^{3}

Vaporization Rate

The vaporization rate (ref. 5) is given by

$$w = \frac{2\pi DM_m rP}{R\overline{T}}\left[2 + 0.6(Sc)^{1/3}(Re)^{1/2}\right]\ln\left(\frac{P}{P - P_v}\right) \tag{A1}$$

which can be expressed for the stated properties by

$$w = 1.51\times10^{-9}r\left[2 + 1.22\times10^{-2}(rPU)^{1/2}\right]\ln\left(\frac{P}{P - P_v}\right) \tag{A2}$$

By neglecting the 2 within the brackets and defining the Reynolds number velocity as

$$U = \left(\Delta\overline{v}^2 + u^2\right)^{1/2} \tag{A3}$$

the vaporization rate can be expressed as

$$w = 0.32\times10^{-5}\left(\frac{\Delta\bar{v}}{100}\right)^{1/2}\left(\frac{r}{100}\right)^{3/2}\left(\frac{P}{\bar{P}}\right)^{1/2}\left[1+\left(\frac{u}{\Delta\bar{v}}\right)^{2}\right]^{1/4}\ln\left(\frac{P}{P-P_v}\right) \tag{A4}$$

Heat Transfer Rate

The heat transfer rate is given by

$$q = 2\pi kr\left[2 + 0.6(Pr)^{1/3}(Re)^{1/2}\right](T_g - T_\ell)Z \tag{A5}$$

where $Z = z/(e^z - 1)$ and $z = \left[w(C_p)_v(T_g - T_\ell)Z\right]/q$. For the stated properties equation (A5) becomes

$$q = 1.65\times10^{-10}r\left[2 + 1.67\times10^{-2}(rPU)^{1/2}\right](T_g - T_\ell)Z \tag{A6}$$

By treating the bracketed term as for vaporization rate and by assuming a constant temperature difference $\bar{T} - T_\ell$ of 4000° R, the heat transfer rate expression becomes

$$q = 1.95\times10^{-3}\left(\frac{\bar{v}}{100}\right)^{1/2}\left(\frac{r}{100}\right)^{3/2}\left(\frac{P}{\bar{P}}\right)^{1/2}\left[1+\left(\frac{u}{\Delta\bar{v}}\right)^{2}\right]^{1/4}Z \tag{A7}$$

Combining the vaporization rate and heat transfer rate expressions to evaluate z gives

$$z = 6.15\ln\left(\frac{P}{P-P_v}\right) \tag{A8}$$

The heat transfer rate expression can be expressed as

$$q = 12\times10^{-3}\left(\frac{\Delta v}{100}\right)^{1/2}\left(\frac{r}{100}\right)^{3/2}\left(\frac{P}{\bar{P}}\right)^{1/2}\frac{\left[1+\left(\frac{u}{\Delta\bar{v}}\right)^{2}\right]^{1/4}\ln\left(\frac{P}{P-P_v}\right)}{\left(\frac{P}{P-P_v}\right)^{6.15}-1} \tag{A9}$$

Mass Balance

The mass balance for a vaporizing drop being replenished by a constant flow rate $\bar{w}$ is given by

$$\frac{dm}{dt} = \bar{w} - w \tag{A10}$$

Heat Balance

The heat balance for a drop where the difference between the sensible heat carried by the vaporizing liquid and by the replenishing liquid is neglected is given by

$$\frac{dH}{dt} = \frac{1}{m}(q - w\lambda) \tag{A11}$$

Normalized Equations

Normalized variables for the vaporization expressions are given by

$$\left.\begin{aligned} w^* &= \frac{w}{\bar{w}} \qquad P_v^* = \frac{P_v}{\bar{P}} \qquad q^* = \frac{q}{\bar{w}H} \qquad P^* = \frac{P}{\bar{P}} \\ m^* &= \frac{m}{\bar{w}} \qquad \lambda^* = \frac{\lambda}{\bar{H}} \qquad H^* = \frac{H}{\bar{H}} \end{aligned}\right\} \tag{A12}$$

where $\bar{w}$ is the vaporization rate of an initial drop size r_o for steady conditions and $\Delta\bar{v}$ = 100 ft/sec as given by

$$\bar{w} = 0.189\times10^{-5}\left(\frac{r_o}{100}\right)^{3/2} \tag{A13}$$

and m is related to the drop radius by

$$m = \frac{4}{3}\pi r^3 \rho_l \tag{A14}$$

With these notations, the vaporization process at a mean chamber pressure of 300 psi is given by the following expressions:

$$w^* = 33 \frac{(\Delta\bar{v}/100)^{1/2}}{(r_o/100)^{3/4}} (P^*)^{1/2}(m^*)^{1/2}\left[1 + \left(\frac{u}{\Delta\bar{v}}\right)^2\right]^{1/4} \ln\left(\frac{P^*}{P^* - P_v^*}\right) \tag{A15}$$

$$q^* = 200 \frac{(\Delta\bar{v}/100)^{1/2}}{(r_o/100)^{3/4}} (P^*)^{1/2}(m^*)^{1/2}\left[1 + \left(\frac{u}{\Delta\bar{v}}\right)^2\right]^{1/4} \frac{\ln\left(\frac{P^*}{P^* - P_v^*}\right)}{\left(\frac{P^*}{P^* - P_v^*}\right)^{6.15} - 1} \tag{A16}$$

$$\frac{dH^*}{dt} = \frac{1}{m}(q^* - w^* \lambda^*) \tag{A17}$$

$$P_v^* = e^{7-(7.8/H^*)} \tag{A18}$$

$$\lambda^* = 0.65 - \left(\frac{1}{2}\right) H^* \tag{A19}$$

APPENDIX B

LINEAR ANALYSIS

In this appendix a transfer function relating perturbations in pressure and vaporization rate is derived by linear analysis.

The normalized equations for the vaporization process given in appendix A are used. The linearized forms of these equations when gas velocity effects are neglected are given by

$$w^{*\prime} = \frac{1}{2} P^{*\prime} + \frac{1}{2} m^{*\prime} - \beta(P^{*\prime} - P_v^{*\prime}) \tag{B1}$$

$$q^{*\prime} = \frac{1}{2} P^{*\prime} + \frac{1}{2} m^{*\prime} - \beta \left(1 - \frac{6\alpha e^{6\alpha}}{e^{6\alpha} - 1}\right)(P^{*\prime} - P_v^{*\prime}) \tag{B2}$$

$$\bar{m}^* m^{*\prime} S = -w^{*\prime} \tag{B3}$$

$$\frac{\bar{H}^*}{\bar{\lambda}^*} \bar{m}^* H^{*\prime} S = q^{*\prime} - \lambda^{*\prime} - w^{*\prime} \tag{B4}$$

$$P_v^{*\prime} = 7.8\, H^{*\prime} \tag{B5}$$

$$\lambda^{*\prime} = \frac{\bar{H}^*/2}{0.65 - (\bar{H}^*/2)} H^{*\prime} \tag{B6}$$

where

$$\beta = \frac{\left(\dfrac{\bar{P}_v^*}{\bar{P}^* - \bar{P}_v^*}\right)}{\ln\left(\dfrac{\bar{P}^*}{\bar{P}^* - \bar{P}_v^*}\right)} \tag{B7}$$

$$\alpha = \ln\left(\frac{\bar{P}^*}{\bar{P}^* - \bar{P}_v^*}\right) \tag{B8}$$

For steady vaporization at a pressure of 300 psia, $\beta = 1.37$, $\alpha = 0.599$, $\bar{H}^* = 1.0$, and $\bar{\lambda}^* = 0.155$.

Evaluating the linearized equations at this condition gives

$$w^{*\prime} = -0.87\ P^{*\prime} + \left(\frac{1}{2}\right) m^{*\prime} + 1.37\ P_v^{*\prime} \tag{B9}$$

$$q^{*\prime} = 4.2\ P^{*\prime} + \left(\frac{1}{2}\right) m^{*\prime} - 3.7\ P_v^{*\prime} \tag{B10}$$

$$\bar{m}^* m^{*\prime} S = -w^{*\prime} \tag{B11}$$

$$6.45\ \bar{m}^* H^{*\prime} S = q^{*\prime} - \lambda^{*\prime} - w^{*\prime} \tag{B12}$$

$$P_v^{*\prime} = 7.8\ H^{*\prime} \tag{B13}$$

$$\lambda^{*\prime} = -3.23\ H^{*\prime} \tag{B14}$$

Combining these equations gives the transfer function

$$\frac{w^{*\prime}}{P^{*\prime}} = 0.622\ \frac{2\ \bar{m}^* S}{1 + 2\ m^* S}\left(\frac{1 - 0.249\ \bar{m}^* S}{1 + 0.178\ \bar{m}^* S}\right) \tag{B15}$$

APPENDIX C

COMPARISON OF VAPORIZATION MODELS

The frequency response properties of the vaporization process reported previously (refs. 2 and 3) were restricted to sinusoidal acoustic oscillations. A comparison with these previous results is made here (1) to bring the present analysis into perspective with the previous studies and (2) to establish a degree of confidence in the specific model and method of evaluation used in this study to examine the effects of wave distortion on response properties.

The single-drop model used in this study attempts to simulate the entire vaporization process in a combustor with its multiplicity of drops and continuous injection. The response of the entire vaporization process to sinusoidal disturbances was evaluated for n-heptane drops in reference 2. Individual heating transients, accelerations, and vaporization histories for each drop within the process were evaluated. Some of the results of that study are shown in figure 11. The average value of the in-phase response factor $\mathcal{R}$ is shown as a function of frequency for variations in drop size, final gas velocity, and pressure amplitude. For each condition there is a frequency for peak response. This frequency increases with a decrease in drop size and with an increase in final gas velocity and pressure amplitude. The peak values of the response factor curves are relatively constant at a value of about 0.7.

Figure 12 shows comparable results obtained for the model and method of analysis used in the present study. (An increase in final gas velocity is comparable to some proportional increase in relative axial Mach number $\Delta\bar{v}/c$.) The peak response, the frequency at which this peak occurs, and the effect of the variables on this peak response frequency are in relatively good agreement with those of reference 2. The model appears to adequately characterize the frequency response properties for the purpose of examining the effect of wave distortion on the response properties.

In reference 3, analytical solutions for the frequency response properties of the vaporization process were derived by linear analysis. Such analytical solutions provide exact values of the response factors for infinitesimal sinusoidal oscillations. The solutions also provide the correlating parameter $\omega\bar{\tau}$ (characteristic frequency) for the response properties. The parameter $\bar{\tau}$ is a characteristic drop lifetime defined by $\bar{m}/\bar{w}$, which for the numerical evaluations of this study is equal to $\bar{m}^*$.

Figure 13 shows the in-phase response factor $\mathcal{R}$ as a function of the characteristic frequency $\omega\bar{\tau}$ obtained both by the linear analysis developed in appendix B and by numerical evaluations. Also shown in figure 13 (lower curve) is the result from the linear analysis of reference 3, where a correction term for simultaneous heat and mass

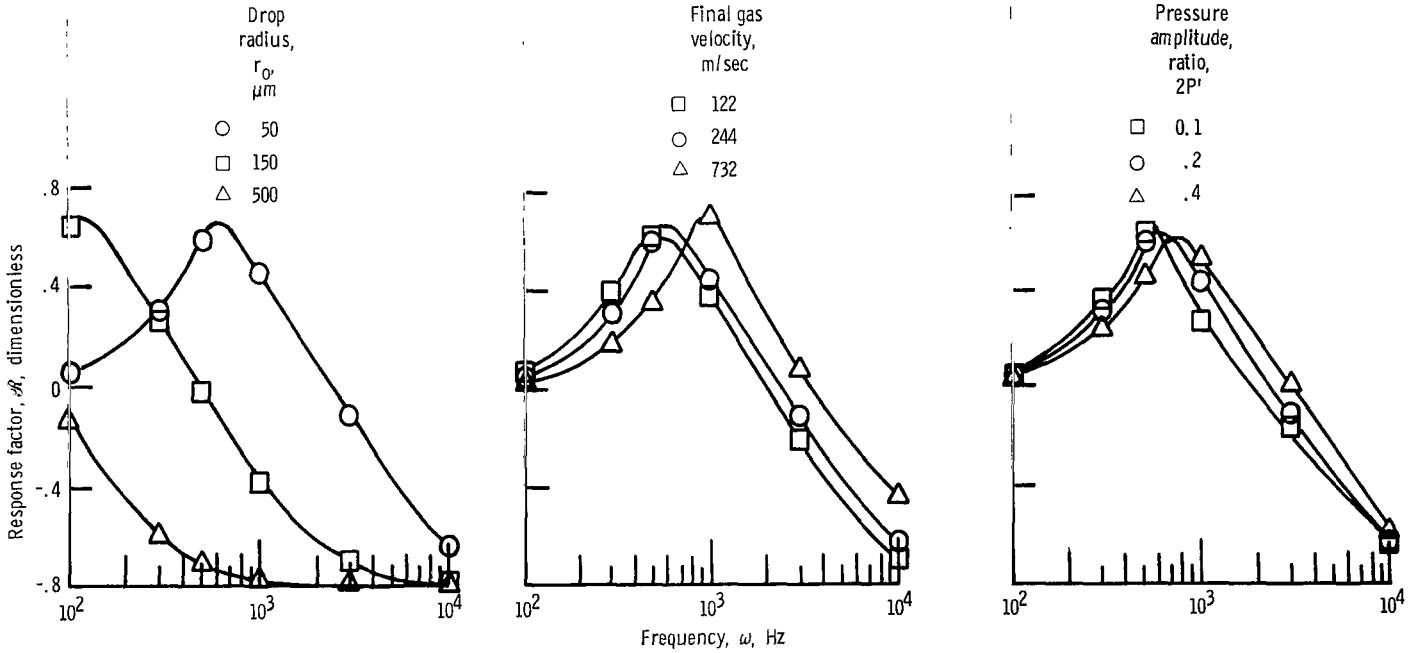

(a) Effect of initial drop radius. Drop conditions: velocity, 30.5 m/sec (100 ft/sec); temperature, 361 K (650° R). Gas conditions: pressure, 2068 kN/m^2 (300 psi); final velocity, 244 m/sec (800 ft/sec); oscillation peak-to-peak amplitude, 0.2 of average gas pressure.

(b) Effect of final gas velocity. Drop conditions: radius, 50 μm; velocity, 30.5 m/sec (100 ft/sec); temperature, 361 K (650° R). Gas conditions: pressure, 2068 kN/m^2 (300 psi); oscillation peak-to-peak amplitude, 0.2 of average gas pressure.

(c) Effect of peak-to-peak pressure amplitude ratio. Drop conditions: radius, 50 μm; velocity, 30.5 m/sec (100 ft/sec); temperature, 361 K (650° R). Gas conditions: pressure, 2068 kN/m^2 (300 psi); final velocity, 244 m/sec (800 ft/sec).

Figure 11. - Frequency response properties from reference 2 obtained with a multiple-drop transient vaporization model.

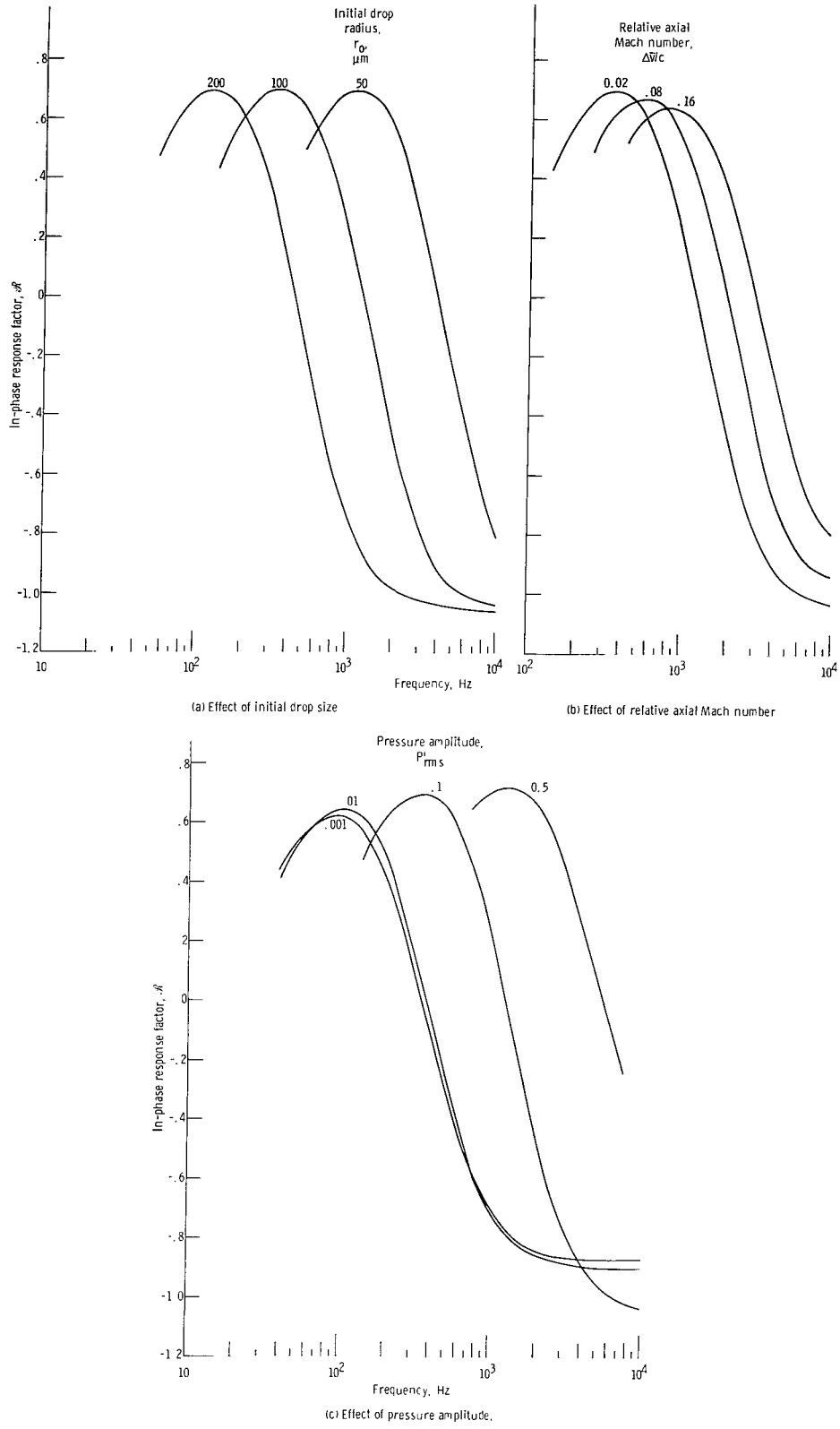

Figure 12 - In-phase response properties for sinusoidal disturbances. Conditions: relative axial Mach number $\Delta\bar{v}/c$, 0.02; pressure amplitude P'_{rms}, 0.1; ratio of harmonic coefficients p_2/p_1, 0.

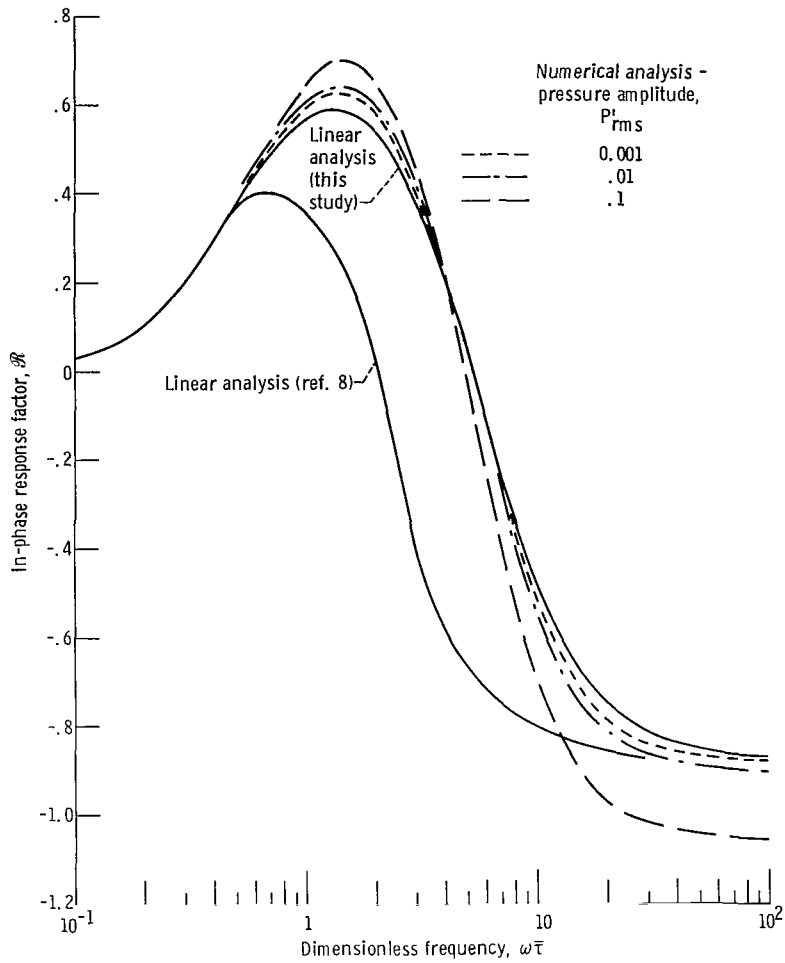

Figure 13. - Comparison of analyses.

transfer and the variation in the heat of vaporization with drop temperatures were neglected. The present linear analysis includes these variables.

A comparison of the two linear analyses shows that the additional variables increase the peak response to a value of about 0.6 and increase the characteristic frequency for peak response to a value of about 1.3. These changes alleviate some of the concern expressed in reference 3 about the magnitude and position of the peak response from that linear analysis.

A comparison of the numerical solutions and the modified linear analysis in figure 3 shows relatively good agreement of the response properties. As pressure amplitude decreases, the numerical response properties converge toward the linear solution. The result gives added confidence in this study to evaluate the response properties.

REFERENCES

1. Heidmann, Marcus F.: Amplification by Wave Distortion of the Dynamic Response of Vaporization Limited Combustion. NASA TN D-6287, 1971.

2. Heidmann, Marcus F.; and Wieber, Paul R.: Analysis of n-Heptane Vaporization in Unstable Combustor with Traveling Transverse Oscillations. NASA TN D-3424, 1966.

3. Heidmann, Marcus F.; and Wieber, Paul R.: Analysis of Frequency Response Characteristics of Propellant Vaporization. NASA TN D-3749, 1966.

4. Priem, Richard J.; and Rice, Edward J.: Combustion Instability with Finite Mach Number Flow and Acoustic Liners. Twelfth Symposium (International) on Combustion. Combustion Inst., 1969, pp. 149-159.

5. Priem, Richard J.; and Heidmann, Marcus F.: Propellant Vaporization as a Design Criterion for Rocket-Engine Combustion Chambers. NASA TR R-67, 1960.

NASA-Langley, 1970 —— 33 E-6761

"The aeronautical and space activities of the United States shall be conducted so as to contribute . . . to the expansion of human knowledge of phenomena in the atmosphere and space. The Administration shall provide for the widest practicable and appropriate dissemination of information concerning its activities and the results thereof."

—NATIONAL AERONAUTICS AND SPACE ACT OF 1958

NASA SCIENTIFIC AND TECHNICAL PUBLICATIONS

TECHNICAL REPORTS: Scientific and technical information considered important, complete, and a lasting contribution to existing knowledge.

TECHNICAL NOTES: Information less broad in scope but nevertheless of importance as a contribution to existing knowledge.

TECHNICAL MEMORANDUMS: Information receiving limited distribution because of preliminary data, security classification, or other reasons.

CONTRACTOR REPORTS: Scientific and technical information generated under a NASA contract or grant and considered an important contribution to existing knowledge.

TECHNICAL TRANSLATIONS: Information published in a foreign language considered to merit NASA distribution in English.

SPECIAL PUBLICATIONS: Information derived from or of value to NASA activities. Publications include conference proceedings, monographs, data compilations, handbooks, sourcebooks, and special bibliographies.

TECHNOLOGY UTILIZATION PUBLICATIONS: Information on technology used by NASA that may be of particular interest in commercial and other non-aerospace applications. Publications include Tech Briefs, Technology Utilization Reports and Technology Surveys.

Details on the availability of these publications may be obtained from:

SCIENTIFIC AND TECHNICAL INFORMATION OFFICE

NATIONAL AERONAUTICS AND SPACE ADMINISTRATION

Washington, D.C. 20546